A Coincidence Study of Strong Field Ionization of Rare Gases

By

James Cryan

In Fulfillment of the Requirements

for Graduation with Distinction

from

The Ohio State University

2007

Abstract

Single and double ionization of an atom in a strong field has been a forefront problem in atomic physics for many years. The coincidence method, which will be described in this thesis, has been used to study the processes for both single and double ionization. This coincidence method is useful in determining the spectrum due to each signal (single and double ionization). Furthermore, this method can and will be used by the DiMauro group to further investigate the interaction of light and matter.

As a result of this project the data collection and analysis tools for the DiMauro group have been revised and updated. This should allow for further advances in strong-field ionization studies. The process of studying these phenomena take a great deal of time, as a result at this current time there is no finalized data to report. However, work is still being done to produce these electron spectra as well as study many things about the spectra which are not currently understood.

Contents

List of Figures

Acknowledgements

I would like to thank first and foremost my thesis advisor, Dr. Louis DiMauro. He has spent a great deal of time helping me with this project. In addition to this project Lou has helped me in applying to and deciding on a graduate school, as well as exploring my interests in strong-field physics. The entire DiMauro group deserves thanks for the things they have taught me. Many of the group members deserve special thanks for the help they have given me on this project: Dr. Pierre Agostini, Cosmin Blaga, Phil Colosimo, Fabrice Catoire, and Kevin Schultz.

Chapter 1

Introduction

1.1 Motivation

The interaction of an isolated atom with an intense electromagnetic field is the basis for one of the forefront problems in atomic physics. Furthermore, ionization of this isolated atom has been very useful in understanding the structure of matter. The coincidence method described here is an extremely useful tool in studying the electron energy spectra resulting from the ionization of an atom by an intense field. Furthermore, upon joining the DiMauro group I was charged with updating and further developing the software to be used in this type of experiment. Although a complete coincidence study would be slightly outside the scope of this type of process, I will present the underlying theory as well as a few preliminary results obtained from the use of the software I have developed. Also, in the next section I will present a current problem the group is working on, where implementing the tools presented here will be invaluable.

1.2 Strong Field Physics Overview

A quasi-classical description for this laser-atom interaction has been developed.[1,7] In this model, the atom undergoes a 3-step process, first, the electron is promoted into the continuum by tunnel ionization which will displace the electron away from the core with

very little kinetic energy.[1] The electron will then propagate under the combined influence of the external field and atomic potential until it escapes or collides with the parent ion one half optical cycle later. While under the influence of the field the electron can gain a maximum of 3.17 U_p, where the pondermotive energy, U_p, is the cycle-averaged kinetic energy of a free electron. Upon returning to the parent ion the electron can be recaptured leading to high-harmonic generation, rescatter elastically off the core and gain up to $10U_p$ of energy, or it can scatter inelastically and free additional electrons.

From this description of the interaction dynamics it is obvious that the pondermotive energy, sometimes referred to as quiver energy, is an important quantity in strong-field physics. U_p in atomic units is given by $I/4\omega^2$, where I and ω are the laser intensity and frequency, respectively.[1] Thus the pondermotive energy scales directly with the square of the wavelength of the laser. Most experiments to date have been conducted using 0.8 μm pulsed Titanium Sapphire lasers. The experiments conducted here however, are done at 2 microns. To give an idea of the scaling of U_p, consider Helium exposed to a 10^{15} W/cm^2, 0.8 μm field, then U_p ~ 60eV, but for 2μm, U_p~ 375 eV. This example stresses the advantage of how increasing the wavelength allows for the study of neutral atoms at extremely high values of U_p.

In addition to the pondermotive potential, another vital quantity to the study of strong field physics is the Keldysh adiabaticity parameter, γ. This parameter is the ratio of the optical frequency to the tunneling frequency.[2] According to the Keldysh theory in the limit $\gamma<<1$, the electron is freed via tunneling through the atomic potential barrier, but for $\gamma>>1$, the ionization is multiphoton.[2] This parameter γ, is defined, $\gamma = (I_p/2U_p)^{1/2}$, where U_p is the pondermotive energy, and I_p is the ionization potential of the atom.[2] By

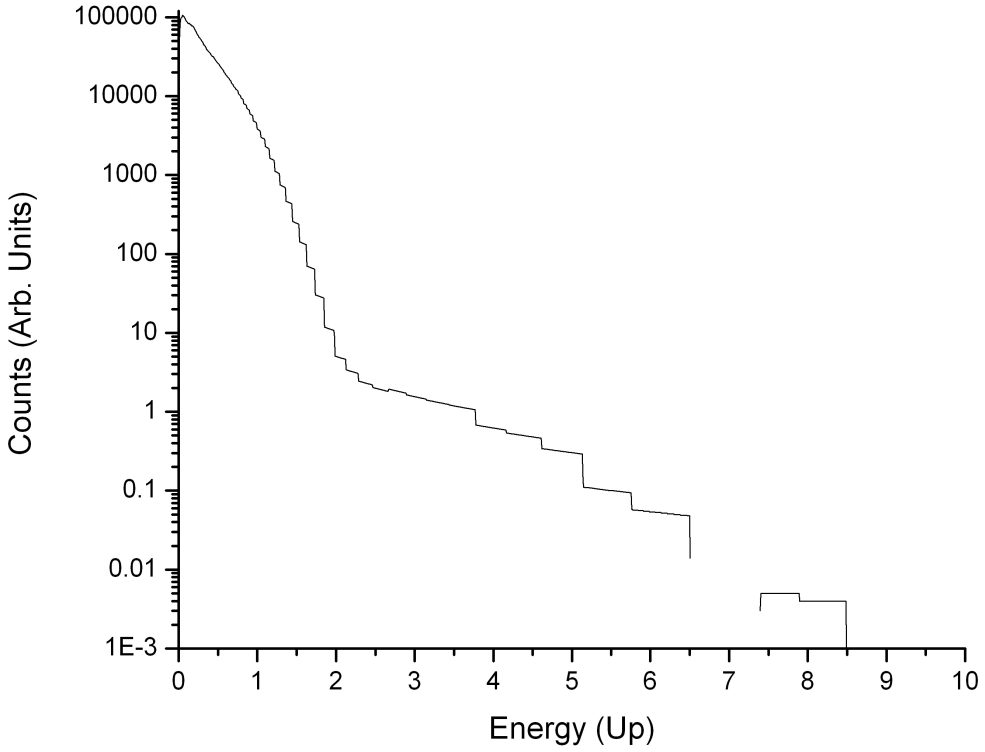

Figure 1 – Photoelectron Energy Spectrum for Argon at 2 μm

increasing U_p as was purposed above allows for deeper investigation into the tunneling regime.

Also, from the description presented at the beginning of the section one can get a general sense of what the photoelectron energy spectrum should look like. Figure 1 shows a photoelectron spectrum for Argon using 2 micron light. The figure shows many important features of the spectrum. First note the drop off towards 2 U_p, which would be expected from the single ionization of the atom, where the electron will not return to or interact with the nucleus. Secondly, Figure 1 shows the plateau region out to 10 U_p, which is the result of the electron rescattering off of the ion core, according to the model

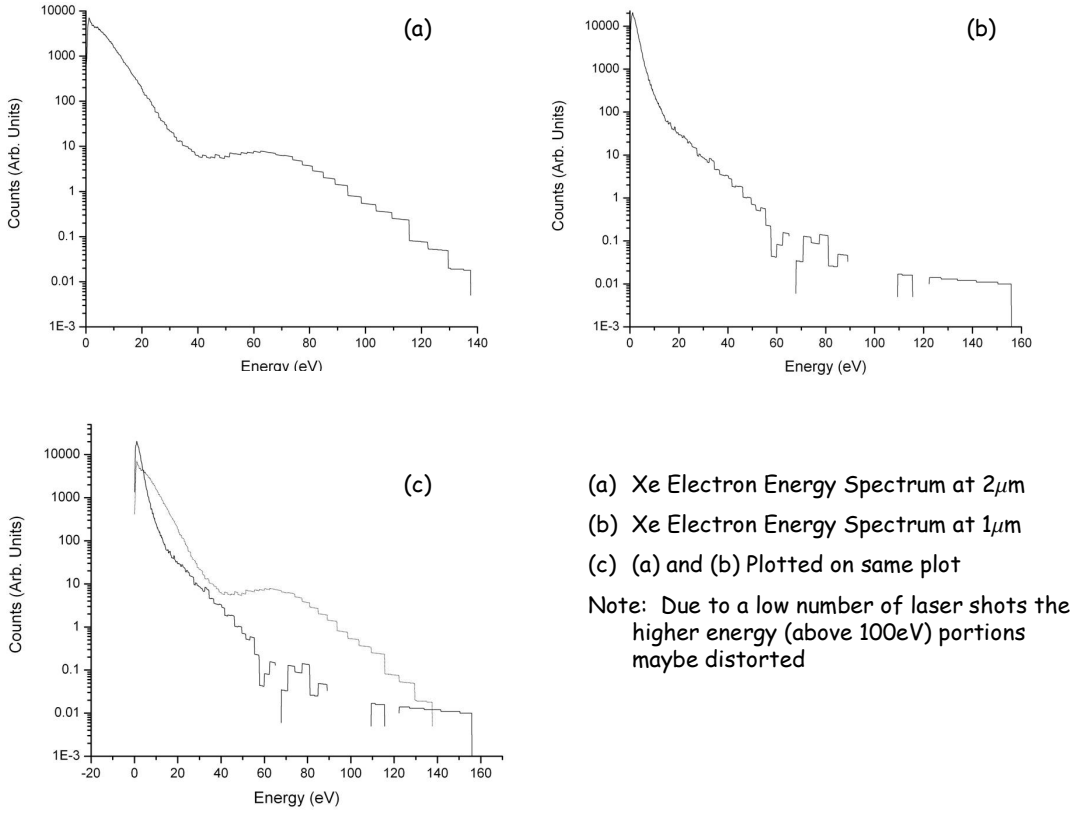

Figure 2 - 1μm and 2μm Electron Energy Spectra for Xenon

presented above. The point where the plateau and the drop features meet has been dubbed the 2 U_p break. One final note for Figure 1, the 'step' appearance of the plateau region is caused by the time resolution of the spectrometer.

Figure 2 shows Xenon photoelectron spectra exposed to (a) 2 microns and (b) 1 micron laser fields. These two spectra show the scaling properties associated with U_p. Notice how the 2 U_p break moves to higher energy as the wavelength increases. The 10 U_p cutoff is impossible to see in Figure 2 however, due to a low number of laser shots.

Another feature seen in Figure 2 is the peak that appears in the plateau region of the 2 micron data. This peak is absent in the 1 micron data. This behavior is quite

strange and is not yet understood. The coincidence method described later is an excellent way to study this behavior. The coincidence study can identify the process responsible for the production of these high energy electrons.

Chapter 2

Coincidence Theory

2.1 Introduction

In this experiment a coincidence event is defined as follows: the detection of a photon (the laser pulse), an ion, and more than one electron. The ion can also be specified to be of a certain charge to mass ratio. When this type of event is recorded, it is tagged as a coincidence event and is then able to be analyzed later. For this type of event it is assumed that the photon detected (or pulse) caused the production of the ion and electrons detected. This data is then useful in discriminating the energy spectrum of electrons created by various ionization processes. As was mentioned earlier, a very interesting and important investigation is the peak seen in the photoelectron spectra at high energy for 2 micron pulses.

2.2 Further Coincidence Discussion

If the electrons are from the ion detected this is referred to as a true coincidence. However, because the detection efficiency of the detectors is not unity, and the interaction volume contains more than one atom, it is easy to see that the electrons and ion may not be from the same event. For example, a double ionization event (formation

of two electrons and one doubly charged ion) occurs and one of the electrons is not detected, instead an electron from a different ionization event is recorded. This type of event has been dubbed a false coincidence. In this type of coincidence experiment, the goal is to maximize the true/false coincidence ratio. In order to accomplish this, the gas pressure and laser intensity are modified. The true/false ratio has been found, theoretically, to be rather good when the ionization rate is very near 1 event per four laser shots. The ion detection rate is slightly smaller than this because of the detection efficiency, and the electron detection is then much lower than this due to the fact that the electron spectrometer has a much lower efficiency. This lower electron detection efficiency is due to the fact that the ions are accelerated toward the MCP, where as the electrons are left to drift under their own kinetic energies, and are collected over a small solid angle. There is a draw back to this type of experiment in that is takes a great deal of time to collect data that will have statistical significance.

2.3 Optimization of Coincidence Rates

As was mentioned earlier in order to collect true coincidences it is necessary to keep the ionization detection (and thus electron and ion detection) rate low. In this section this statement will be elaborated on. For the purpose of this discussion we will consider only a single ionization event which is defined as the detection of one ion and one electron. In this case we will define the mean number of single ionizations per laser pulse $\bar{n}$. In order to start the discussion we assume that all electrons and ions detected are from the photoionzation process. Both channels (electrons and ions) will have losses due to less than perfect detectors, the angular acceptance of the spectrometers, and

collisions which may occur in the interaction region. This means that the number of ion and electrons detected is

$$w_{e(i)} = \xi_{e(i)}\, \bar{n} \tag{2.1}$$

where, $w_{e(i)}$ is the number of electrons or ions, and $\xi_{e(i)}$ is the detection efficiency of the electrons or ions, which includes the factors listed above (small acceptance angle, collisions, and detector efficiencies).[3] Further more, the number of ionization events per laser pulse is described by a Poisson distribution,

$$p(n) = \frac{\bar{n}^n}{n!} e^{-\bar{n}} \tag{2.2}$$

where, p(n) is the probability of having n ionization events.[3] If n electrons (ions) are created by each laser pulse the probability of detecting k of them is governed by the binomial distribution such that,

$$p_{e(i)}(n, k) = \binom{n}{k} \xi_{e(i)} (1 - \xi_{e(i)})^{n-k} \tag{2.3}$$

where, $p_{e(i)}(n,k)$ is the probability and $\xi_{e(i)}$ is again the efficency.[3] The probability, w_{11}, of detecting one ion and one electron is then given by summing the expression $p_e(n,1)p_i(n,1)p(n)$ (the probabilities are simply multiplied because the detections are independent events) over all values of n.[3] The result of this sum is given by,

$$\begin{aligned} w_{11} = {} & \xi_i \xi_e \bar{n}[1 + \bar{n}(1 - \xi_e)(1 - \xi_i)] \\ & \times \mathrm{Exp}\{-\bar{n} + \bar{n}(1 - \xi_e)(1 - \xi_i)\} \end{aligned} \tag{2.4}.$$

This expression gives the total number (true and false) coincidences for each laser shot. According to [3], out of the n pairs created, the probability of detecting the ion and electron from the same ionization event is 1/n, and then the number of true coincidences w^t_{11} becomes,

$$w^t_{11} = \xi_i \xi_e \bar{n}\, \mathrm{Exp}\{-\bar{n} + \bar{n}(1 - \xi_e)(1 - \xi_i)\} \tag{2.5}.$$

Likewise, the number of false coincidences, is merely the number of coincidence events minus the number of true coincidences or,

$$w^{f}_{11} = \xi_i \xi_e \bar{n}^2 (1 - \xi_e)(1 - \xi_i) \times \mathrm{Exp}\{-\bar{n} + \bar{n}(1 - \xi_e)(1 - \xi_i)\} \quad (2.6).$$

Finally, we can look at the maximum in the number of true coincidences given by,

$$w^{max}_{11} = \xi_i \xi_e e^{-1}[1 - (1 - \xi_e)(1 - \xi_i)]^{-1} \quad (2.7).$$

It is important to note the dependence of the number of true and false coincidences on the efficiencies. As will be shown later the detection efficiencies of the electron and ion spectrometers are rather low, however if either detection efficiency were unity (this includes the detector as well as the considerations mentioned before), there would be no false coincidences. The discussion in [3] goes on to point out that the total number of electrons, ions, and coincidences can be determined experimentally and given the expressions above, the efficiencies, and mean number of ionizations can be determined. Conversely, given the efficiencies, the average number of ionizations can be adjusted to maximize the ratio of true coincidences to total coincidences. The dependence of the total (w_{11}), true (w^{t}_{11}), and false (w^{f}_{11}) coincidence rates on the average number of ionization events is shown in Figure 3. Here the values used for ξi and ξe are 0.3 and 0.01 respectively. These values are very close to the values of the apparatus used in the experiment. Consider the maximum rate of true coincidence which is given by equation 2.7, and can be seen in Figure 3, for this ionization rate, the true to false ratio is very poor, near 0.44. However, if the ionization rate decreases to 0.25 (one ionization every four laser shots), the true/false ratio is much better, near 5.8. Continuing to decrease the ionization will increase the true/false ratio, however it will also decrease the total coincidence rate. As the coincidence rate decreases, the number of laser shots required to

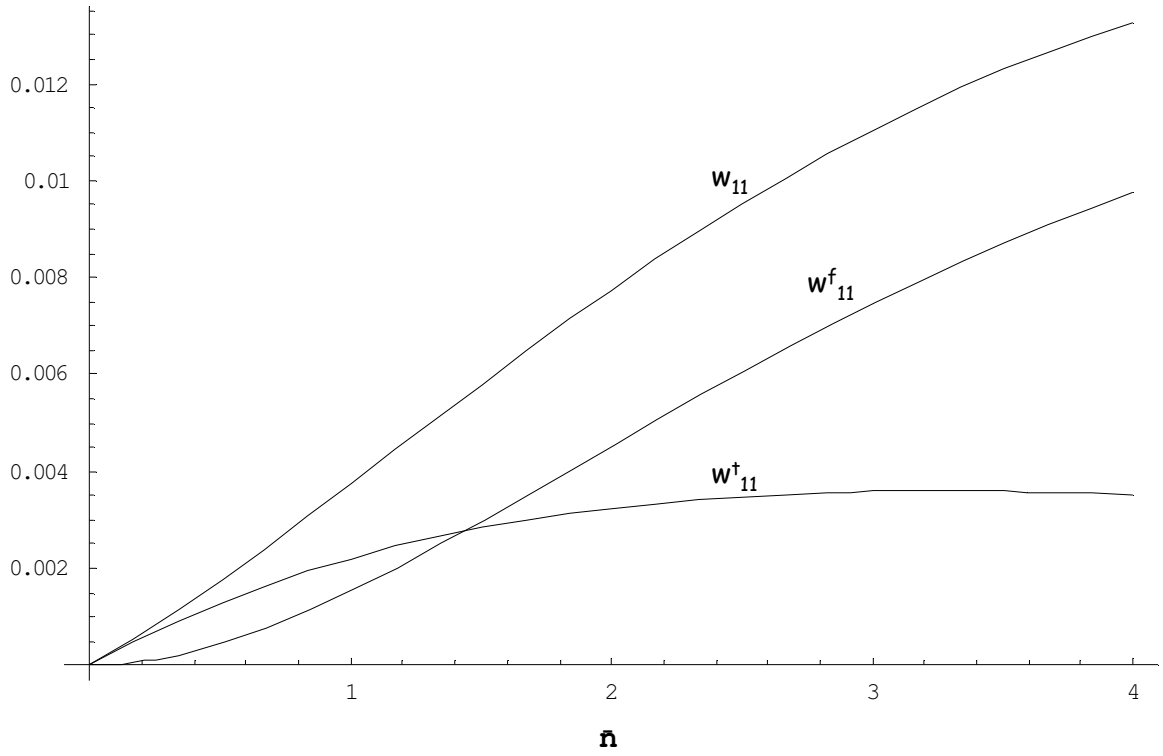

Figure 3 - Coincidence Rates as a Function of Ionization Rate with ξi=0.3 and ξe=0.01

observe a large number of coincidences increases, and so will the total time needed to run the experiment. For this reason the experiments will be conducted with an ionization rate of one event every four laser shots.

Chapter 3

Experimental Setup

3.1 Laser System

As described in the introduction, the study of strong field physics is driven by the availability of lasers which can generate these intense fields. One way to achieve the high intensities necessary is through using short pulses. For a short pulse smaller amounts of energy will result in large peak powers of the pulses. Producing short pulses has become a common practice, and these very short pulses have been achieved using Titanium Sapphire (Ti:Saph) crystals as the gain medium.

These short pulses can be made more energetic using an amplifying scheme deemed chirped pulse amplification (CPA).[6] This method stretches the short pulses in time to reduce the peak intensity and then after amplification, the pulses are compressed.[6] This type of system is necessary because direct amplification of such short pulses would lead to optical damage of gain medium due to extreme peak powers.

The laser used in this experiment is rather unique, it produces 400 mW at 1 kHz for 50 fs pulses of 2000 nm wavelength. In order to create this type of pulse many different processes must be exploited.

The process of creating this light begins with an 8 fs Ti:Saph oscillator (Venteon Pulse 1), this oscillator is pumped by a 532 nm green laser (Spectra-Physics Millennia V). The pulse produced is 0.2 mJ, extremely short, and the central wavelength is near 800 nm. This short pulse is then stretched to 230 ps, before the beginning of the amplification process. The stretcher consists of two gratings which will temporally separate the different colors in the pulse. This stretched pulse serves as the seed for a regenerative amplifier (REGEN).

The pulse enters the REGEN and is then trapped using a Pockels cell. In the REGEN the pulse is amplified by a Ti:Saph crystal pumped by a 532 nm laser (Quantronix Falcon 527). While in the REGEN the pulse is monitored by a photodiode. Once the pulse has been sufficiently amplified the REGEN cavity is dumped and the amplified pulse then enters a multi-pass amplifier. The time the pulse spends in the REGEN determines the repetition rate of the laser, which is 1 kHz.

In the multi-pass amplifier, the pulse takes two more passes through a Ti:Saph crystal which is pumped by another 532nm laser (Quantronix Darwin). From the multi-pass amplifier, the amplified pulse is compressed by two gratings, in much the same way as the stretcher works.

After being compressed the pulse is around 50 fs. This pulse then undergoes a parametric amplification process in the TOPAS (by Light Conversion). The resulting pulse is the one described in the beginning of this section, and is then transported to the interaction chamber.

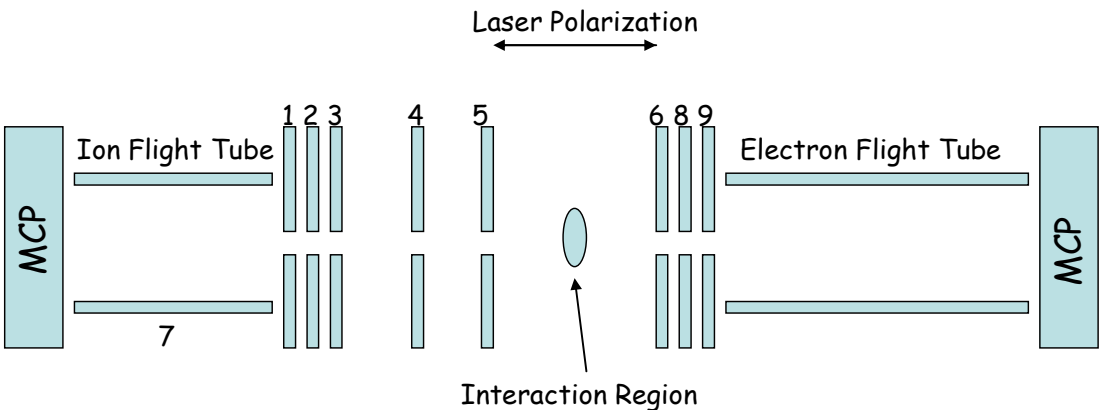

Figure 4 – Schematic view of coincidence spectrometer

3.2 The Spectrometers

The light produced by the laser is then used to ionize the gas of interest. The interaction occurs in a vacuum chamber, and the interaction region is sandwiched between two spectrometers. A schematic view of the spectrometer can be seen in Figure 4. As one can see there is an electron time of flight spectrometer on one side, and an ion mass spectrometer on the other.[8] The design allows for the electrons to be measured by a field free time of flight method, where as the ions are accelerated towards the detector, in order to achieve a greater collection efficiency.[8]

The collection begins when the laser pulse arrives at the final turning mirror. The bleed through of the mirror is detected by a photodiode. After this final mirror, the laser pulse will ionize the gas in the interaction region. The electrons are allowed to propagate away from the interaction region and into the time of flight spectrometer. After the electrons have had sufficient time to enter the flight tube, extraction voltages are turned on to accelerate the ions into the mass spectrometer. This sequence is repeated at the repetition rate of the laser which was 1 kHz.

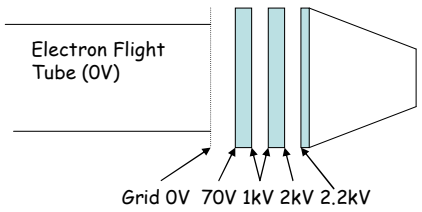

Figure 5 – Schematic view of MCP plate assembly From [6]

3.2.1 The Electron Spectrometer

The electron time of flight spectrometer is shielded from electric and magnetic fields by plate 9 in Figure 4. From the initial ionization event, the electron will drift under its own kinetic energy to the MCP at the end of flight tube. The energy of an electron is given by,

$$E = \frac{m_e L^2}{2 T_{tof}^2} , \tag{3.1}$$

where, L is the effective length of the time of flight tube, and the T_{tof} is the measured time of flight. Given this expression it is obvious that the relationship between energy and time of flight is not linear. For this reason certain considerations, which will be discussed later, must be given in the conversion process from time of flight to energy.

The electron flight tube was designed in order to maximize resolution and collection angle. The acceptance full angle of the spectrometer is 11 degrees. The MCP which detects the electrons, is shown in a schematic view in Figure 5. The flight tube is then shielded from these voltages by a wire mesh in front of the MCP plates. The flight tube is also shielded from the earth's magnetic field by a μ-metal shield.

A final point of discussion is the efficiency of this spectrometer. As is apparent from previous discussion the electrons are preferentially directed along the axis of polarization of the laser.[5] However, there is no preference in direction beyond this, which means that at very best only 50% of the ejected electrons could be detected.

However, the small acceptance angle, and efficiency of the MCP plates will further reduce the overall efficiency of the spectrometer to 1%.[4]

3.2.2 The Ion Spectrometer

Figure 4 clearly shows that that ion spectrometer consists of 6 plates. The plates labeled 1-3 in the figure, act as an electrostatic lens to focus the ions into the MCP detector.[4] Plate 7, is the ion flight tube itself, and is kept grounded. Plates 5 and 8 in the figure are the extraction plates. A voltage is put on plate 5 in order to accelerate the ions into the flight tube. Plate 8 is put at a voltage twice that of plate 5 in order to block secondary electrons from entering the electron spectrometer. Finally, as mentioned previously, plate 9 is grounded to isolate the electron flight tube from any field.

The extraction plates can be operated in two different modes. In order to achieve greater resolution with the spectrometer plates 5 and 8 can be kept at a constant voltage through out the entire interaction time and extract ions as soon as they are created. The second mode is used when ions and electrons from a single shot are to be collected. The interaction is allowed to occur with plates 5, 6, and 8 grounded, to allow the electron to propagate to the shielded time of flight tube. Then the extraction plates are pulsed on, to accelerate the ion into the detector. The electrons are given 400 ns to propagate before the extraction plates are pulsed. Almost no ions are lost in this waiting period, because the recoil energy of the ions (from the laser interaction) is very small. The largest factor for reducing the ion energy resolution is the thermal energy of the ions, which is an order of magnitude larger than the recoil energy.[4]

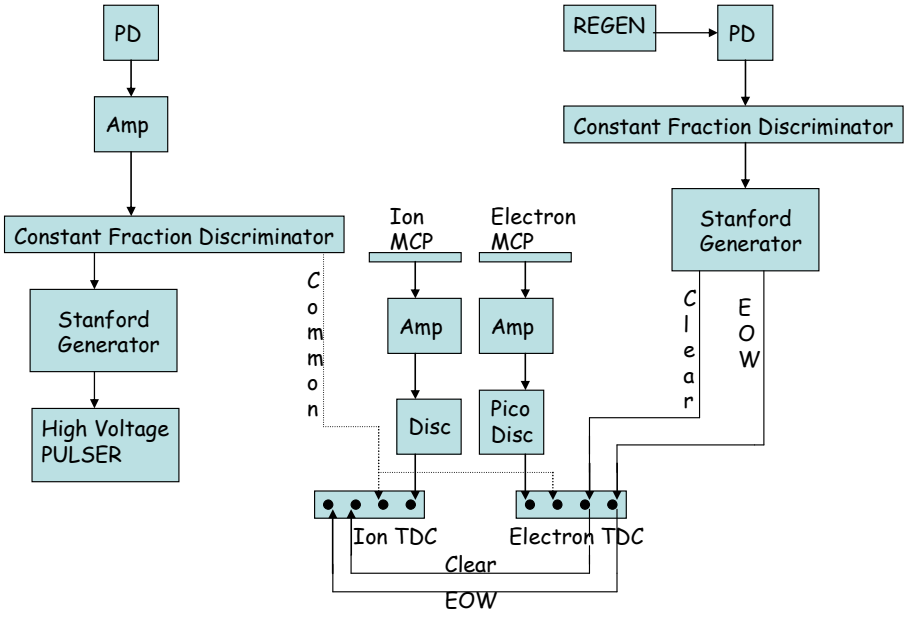

Figure 6 – Schematic diagram of data acquisition electronics

The exact voltages placed on the plates for extraction are chosen to maximize the detection efficiency of the ions.

3.3 Data Acquisition

As was discussed in the previous section about the laser system, the pulse in the REGEN is monitored by a photodiode. The signal form this photodiode is sent to a delay/pulse generator (Stanford Research System DG-535), which is used to generate the 'Clear' and 'End of Window' signals for the time to digital converter (TDC, LeCroy 4208). Another photodiode is positioned at the final turning mirror before the chamber. The signal from this photodiode is sent to a timing amplifier (Ortec 547) and then to a constant fraction discriminator (Ortec 437A). The signal from the discriminator is split and one signal is sent to the TDC 'Common' (which defines zero time). The other output of the discriminator is connected to another delay/pulse generator, which generates the

trigger pulse (delayed 400 ns) for the high voltage pulser which changes the voltage on plates 5 and 8. The schematic diagram of this layout can be seen in Figure 6.

The electron and ion signals generated by the MCP plates are sent to an amplifier and then a discriminator (Ortec 9307 – electron, LeCroy 620D – ion) before reaching the TDC 'Stop'. These connections are also shown in Figure 6.

The time of flight data is read by the TDC, and converted to a digital signal. The data is the transferred to the computer by a CAMAC module. The data is read out using

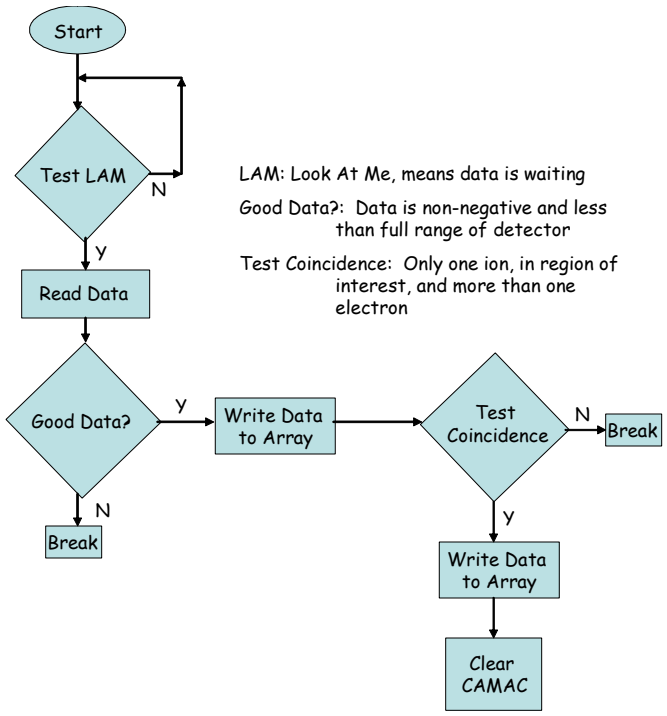

Figure 7 - Data Collection Program Block Diagram

a program called JPC Read TDC. A block diagram of this program is shown in Figure 7.

3.4 Energy Conversion Procedure

As was seen earlier the conversion between time of flight and energy is not linear. In order to deal with this conversion a program (tof to eng convert) was written to convert the raw time of flight data to energy.

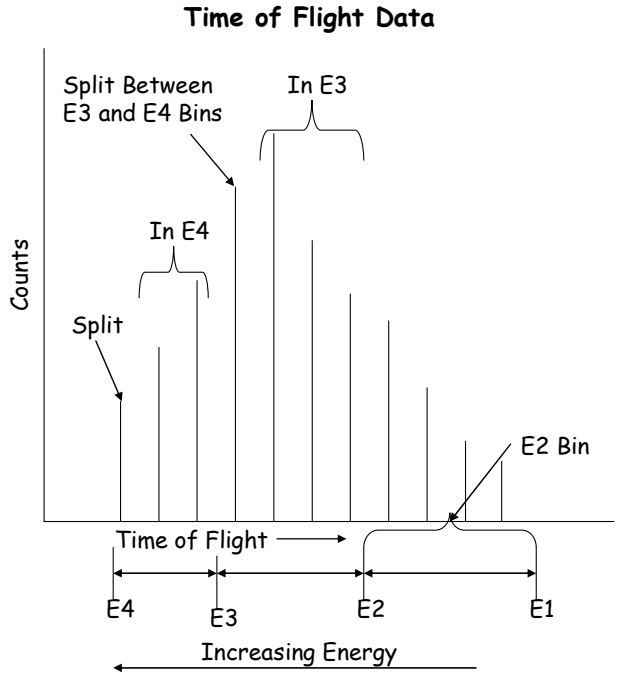

Figure 8 - Schematic of Energy Conversion

The time of flight data is collected by a TDC which collects the data in 1ns bins. All counts in 1 ns are placed in the same bin. This data needs to be converted to an energy spectrum, which should have equal energy bins.

The procedure for this conversion is as follows. The size of an energy bin is determined from the maximum energy and the desired number of bins. For each energy bin, the bin is denoted by its upper bound, i.e. electrons with energy E_1 to E_2 are placed in the bin labeled E_2. Next the upper and lower bounds (E_2 and E_1) are converted to time of flights using equation 3.1. The idea is that all electrons with a time of flight between these two times belong in the same energy bin. However, the bounds of an energy bin do not occur exactly at the ends of the time bins, so some time bins need to be divided between two energy bins. This procedure is shown schematically in Figure 8. The time bin with the arrow in Figure 8 will be split between the two adjacent energy bins based

on where the bound of the energy bin lies in time. After this process, the resulting energy spectra will have equal energy bins, and can be viewed on a linear energy scale.

The treatment of the coincidence experiments was discussed earlier. Based on this discussion, the program 'scatter' was written and used to analyze the coincidence data. The program creates time of flight data electron spectra for each ion of interest. The program also calculates the true: false ratio from the known collection efficiencies. The time of flight spectra can then be converted to energy using the program described previously.

Chapter 4

Results

4.1 Results

The goal of this project was to develop the data collection program (JPC Read TDC) for use with the experimental apparatus described in chapter 3. Another goal of this project was to develop data analysis tools (convert tof to eng and scatter) using the method described in chapter 2 as well as the end of chapter 3. These goals have been met by this time. The results of the data collection and analysis programs are exhibited in Figures 1 and 2. This data was collected and analyzed using the programs created as a result of this project. The coincidence analysis program has also been tested and been shown to be in working condition.

However, at this time there are no results from this sort of analysis. The coincidence program will be used to analyze data to help understand the peak in the energy spectrum that is described in chapter 1. This study is proving to be quite a task, and the time required for this type study is defiantly beyond the scope of this type of project.

Given this problem, that no coincidence data has been deemed worthy of publication, the project is still a success. The data acquisition and analysis programs have been proven to work, which is the main goal of this project.

References

1. K.J. Schafer, B. Yang, L.F. DiMauro and K.C. Kulander, "*Above threshold ionization beyond the high harmonic cutoff*", Phys. Rev. Lett. **70**, 1599 (1993).
2. L. V. Keldysh, "*Ionization in the filed of a strong electromagnetic wave*", Zh. Eksp. Teor. Fiz. **47**, 1945 (1964). [Sov. Phys. JETP **20**, 1307 (1965).]
3. V. Stert, W. Radloff, C.P. Schulz, and I.V. Hertel, *"Ultrafast photoelectron spectroscopy: Femtosecond pump-probe coincidence detection of ammonia cluster ions and electrons"*, Eur. Phys. J. D **5**, 97-106 (1999).
4. J. Rudati, *"A Study of Strong Field Double Ionization of Rare Gases"* (2003).
5. T.J. McIrath, P.H. Bucksbaum, R.R. Freeman, and M. Bashkansky, *Ábove-Threshold Ionization Process in Xenon and Krypton"*, Phys. Rev. A **35(11)**, 4611-4623 (1987).
6. D. Strickland and G. Mourov, "*Compression of amplified chirped optical pulses*", Opt. Commun. **56**, 219 (1985).
7. P.B. Corkum, *"Plasma Perspective On Strong-Field Multiphoton Ionizations"*, Phys. Rev. Lett., **71(31)**, (1993).
8. R. Lafron, J.L. Chaloupka, B. Sheeny, P.M. Paul, P. Agostini, K.C. Kulander, and L.F. Dimauro, *"Electron Energy Spectra from Intense Laser Double Ionization of Helium"*, Phys. Rev. Lett., **86(13)**, 2762-2765 (2001).